ELSEVIER

PII: S0032-3861(98)00109-8

Polymer Vol. 39 No. 26, pp. 7067–7077, 1998

0032-3861/98/$ - see front matter

Microstructure development during constant-force drawing of poly(ethylene terephthalate) film*

D. R. Salem
TRI/Princeton, P.O. Box 625, 601 Prospect Ave., Princeton, NJ 08542, USA
(Received 6 January 1998; accepted 28 January 1998)

Structure development in PET film during high strain-rate, constant-force (CF) deformation in the temperature range 80–96°C is compared with structure development during lower strain rate, constant-extension-rate (CER) deformation in a similar temperature range. The higher (maximum) strain rates involved in CF drawing mean that much of the deformation takes place in a regime where the time available for orientational relaxation and crystallization is short. This results in high levels of 'non-crystalline orientation' and low levels of crystallinity compared to structures obtained from CER drawing. In CER drawing, due to the lower strain rates, the degree of crystallinity always has time to reach pseudo-equilibrium values corresponding to a given level of non-crystalline orientation, and the amount of orientational relaxation occurring during drawing has the dominant influence on structure development. In CF drawing, pseudo-equilibrium crystallinity values are not reached, except when the deformation approaches the tail-end of the strain-rate spectrum. The results also provide confirmation that microstructure data obtained from rapidly quenched samples are consistent with microstructure data obtained from real-time experiments.

(Keywords: poly(ethylene terephthalate) film; constant-force drawing; microstructure development)

INTRODUCTION

In most laboratory studies of microstructure development during hot-drawing of PET film, the film samples were drawn at a constant rate of extension. During this type of deformation the strain rate continuously decreases from its nominal value, according to the relationship indicated in *Figure 1*. Typically, the force applied to the film during constant-extension-rate (CER) drawing increases in two stages, reflecting the deformation of the entanglement network and stress-induced microstructural changes [1–8] (*Figure 2*). A few studies of constant-strain-rate (CSR) drawing have also been made, in which the rate of extension is continuously increased to maintain a given strain rate [9,10], and a similar stress–strain response would be expected in this mode of deformation.

Although CER deformation is used in the manufacture of PET film (tenter drawing), the commercial processes most widely used involve drawing between rolls. This is a constant-force (CF) deformation, in which the draw ratio is defined by the ratio of the speed of the second (fast) roller to that of the first (slow) roller. The residence time of the film in the 'draw gap' is determined by the distance between the rolls and their speed. A reasonable laboratory simulation of drawing between rolls is deformation under a (high) constant load, i.e. a creep experiment at high strain rate. It has been found that constant-load drawing of amorphous PET film involves an increasing rate of strain in the early part of the deformation, followed by a decreasing strain rate in the final stages of deformation [11], shown schematically in *Figure 3*. Based on the work of Lorentz and Tassin [12], and our own studies, we believe that molecular relaxation in the early stages of constant-load drawing, where strain rate is relatively low, results in a decreasing entanglement network density which leads to reduced resistance to deformation and rapidly increasing strain rate. The onset of orientation-induced crystallization in the course of the deformation increases the modulus of the polymer by providing fixed network junction points and causes the strain rate to decrease again.

Since the force associated with a particular set of roll-drawing conditions is unknown and the strain-rate history is complex, analysis of CF deformation is difficult. Laboratory simulation of roll drawing, in which PET film was stretched under a dead weight, has provided information on the evolution of strain rate during drawing and its dependence on draw temperature and microstructure development [11,13], and there has also been a qualitative description of the relaxation phenomena occurring [12]. However, the literature on CF drawing of PET film remains relatively sparse, and little is understood about e.g. the factors controlling crystallization onset and crystallinity development in this mode of deformation. By contrast, detailed data have now been acquired on microstructural development and crystallization kinetics during CER and CSR drawing of PET film, including the influence of strain rate [6,9,10,14–20], draw temperature [3,9,10,17–20] and molecular weight [21].

In the present study, we compare microstructural data obtained from roll-drawn film, produced on an industrial pilot plant under various temperature and strain-rate conditions, with some of our previous data obtained from CER drawing on a laboratory scale [6,14–19]. We have found that the understanding elicited from our studies of CER drawing of PET film has helped to elucidate the nature of process–structure relationships in CF drawing. Through improved understanding of the interplay between the kinetics of deformation, and crystallization and orientational relaxation, we have shown, e.g. the manner in which both crystallization and orientational relaxation are limited

* An abbreviated version of this paper was presented at the SPE Annual Technical Conference, 6–10 May 1996, Indianapolis, Indiana, USA.

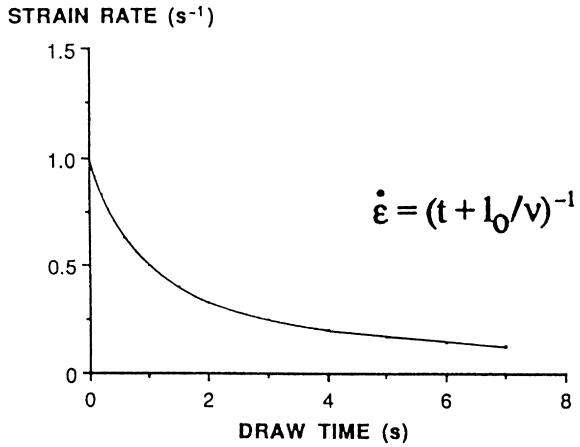

Figure 1 Changes in strain rate $\dot{\epsilon}$ during constant-extension-rate (CER) drawing, which depend on draw time, t, extension rate, ν and initial gauge length, l_0. The nominal strain rate in this example is 1 s^{-1}.

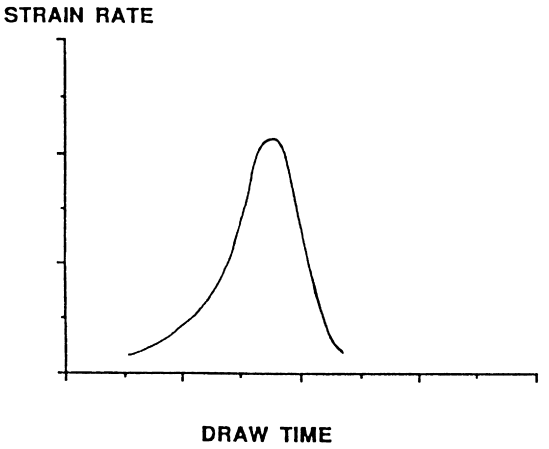

Figure 3 Schematic example of the changes in strain rate during constant load drawing of PET film above T_g [11].

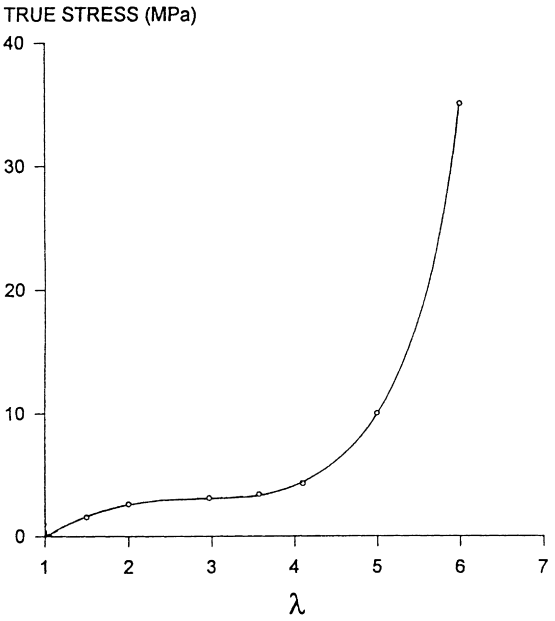

Figure 2 An example of the stress–strain response of (initially) amorphous PET film for CER drawing at temperatures above T_g. The draw temperature was 90°C and the nominal strain rate was 0.01 s^{-1} [6].

by the timescale of the deformation, and the implications of this for structure evolution in both CF and CER drawing.

EXPERIMENTAL

Materials and deformation

Roll-drawn (CF) film. Unfilled sheets of amorphous PET film were cast and roll drawn by Hoechst Diafoil on a pilot line. Samples were produced at draw temperatures of 83, 90 and 96ºC to draw ratios in the range 1.5–4.0. Quenching of the film occurred immediately after drawing by contact with the fast (chill) roll. The main objective was to produce, at each draw temperature, samples with (average) strain rates, $\dot{\epsilon}$, of 5 and 17 s^{-1}. To achieve this, the line speed was decreased as the draw ratio increased. In addition, some samples were produced at lower strain rates by maintaining a constant line speed at all draw ratios. A complete list of samples produced at each draw temperature is given in *Table 1*. The cast film has an intrinsic viscosity of 0.61 dl/g and a density of 1337.8 kg/m^3. All specimens used for microstructural analysis were taken from the centre of the sheets.

Table 1 Drawing conditions of roll-drawn (CF) film

Draw ratio	$\dot{\epsilon}$ (s^{-1})	$\dot{\epsilon}$ (s^{-1})	$\dot{\epsilon}$ (s^{-1})
1.5	—	1.1	—
2.0	5	2.0	17
2.5	5	2.8	17
3.0	5	3.6	17
3.5	5	4.3	17
4.0	5	5	17

Instron-drawn (CER) film. Unfilled, cast sheets of amorphous PET film, supplied by Goodyear, were drawn at constant width (with the exception noted later) in the furnace of an Instron tensile tester. The CER deformation was performed at various nominal strain rates and draw temperatures. At the end of drawing, the samples were immediately air-quenched. The specimen geometry and further details of the deformation procedure were described in our previous study [6]. The cast film has an intrinsic viscosity of 0.61 dl/g and a density of 1339 kg/m^3. Exceptions to constant-width drawing were the samples used to obtain *Figure 18*. Due to a lack of non-crystalline orientation data for constant-width samples drawn at 83 and 96ºC, the data in *Figure 18* were obtained from samples drawn unrestrained, in uniaxial extension (see Refs 15 and 16).

Crystallinity from density

The density, ρ, of the film specimens was measured at 23ºC in a density gradient column containing *n*-heptane and carbon tetrachloride. The volume fraction crystallinity, χ, was estimated from the usual relationship (see, e.g. Ref. 6) using a value for the crystalline density, ρ_c, of 1457 kg/m^3. It is recognized that crystalline density can sometimes vary [21–24], but measurement of lattice spacings by X-ray diffraction indicates that it does not do so under the range of crystallization conditions applied in the present study. The value for the amorphous density, ρ_a, was taken as the measured density of the undrawn film (see figures 11 and 12a of Ref. 6). Based on the estimation of Nobbs et al. [25] and on our own experimental evidence [26], we would not expect orientation in the non-crystalline regions to influence the value of ρ_a unless the degree of non-crystalline ('amorphous') orientation were to exceed 0.45, which it

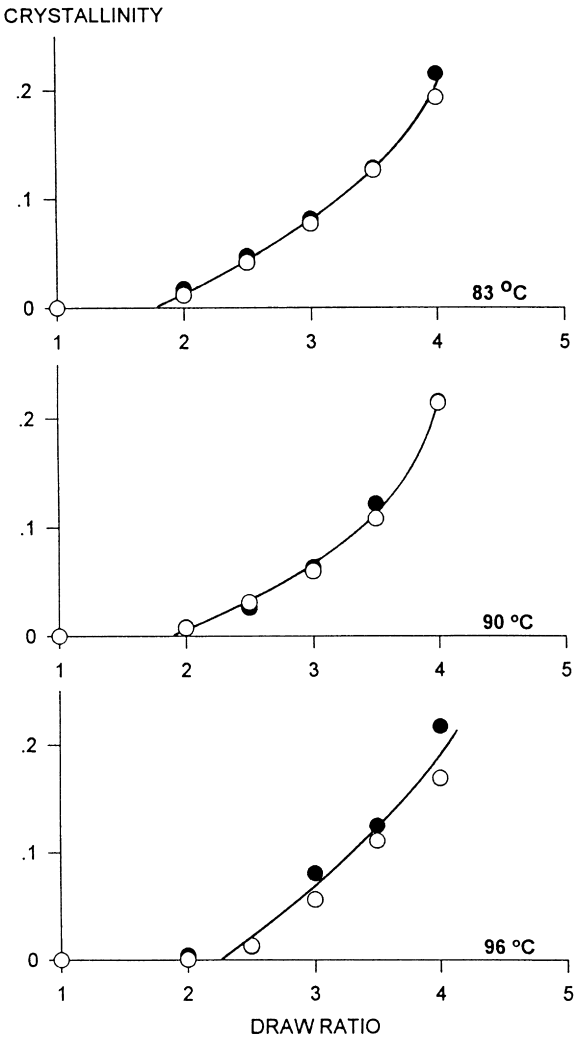

Figure 4 Volume fraction crystallinity as a function of draw ratio for CF-drawn (roll-drawn) film at three draw temperatures, and at (average) strain rates of 5 s^{-1} (●) and 17 s^{-1} (○).

rarely does in the present study. The values of χ that will be reported represent an average of at least three density determinations.

Orientation in the non-crystalline regions from chain-intrinsic fluorescence

The polarized chain-intrinsic fluorescence method for determining molecular orientation in the non-crystalline regions of PET has been described in detail elsewhere [15]. In the present study, the fluorescence emission intensities, I_{ij}, for one-way drawn specimens (along X_3) were measured with the polarizer along X_i and the analyzer along X_j to obtain I_{33}, $I_{31} = I_{13}$ and I_{11}. Using the normalization condition $I_{33} + 4I_{31} + (8/3)I_{11} = 1$, the second moment of the orientation distribution $\langle P_2(\cos\theta)\rangle_{a/fl}$ was obtained [see equation (9), Ref. 15]. It should be emphasized, however, that the roll-drawn samples and constant-width Instron-drawn samples possess some degree of planar orientation, such that the plane of the benzene rings tends to lie parallel to the film surface. This lack of cylindrical symmetry means that the $\langle P_2(\cos\theta)\rangle_{a/fl}$ values in these samples represent the in-plane axial orientation of the uncrystallized chains; they do not describe the orientation distribution in the thickness direction of the film. It may be noted that 'amorphous orientation' and 'non-crystalline orientation' are both abbreviations for molecular orientation in the non-crystalline phase, and in the present paper we have tended to favour the latter term.

Crystallite size from wide angle X-ray scattering

Wide-angle X-ray scattering (WAXS) analysis was performed with a Philips diffractometer in the transmission mode, using crystal-monochromatized CuKα radiation. Equatorial scans were made in the range 8–40°, with intensity data collected every 0.1° for a period of 10 s. A mathematical profile-fitting procedure was used to obtain peak 'half-widths' (full width at half peak maximum) for calculation of crystallite size. The procedure is similar to that of Heuvel et al. [27], in which each of the four equatorial reflections (010, 110, 100 and amorphous) is described by a Pearson VII function.

Specimens drawn at constant width lack cylindrical symmetry: the crystallites have planar as well as axial orientation, with the 100 planes tending to align parallel to the film surface. Consequently, when the equatorial scan is made with the X-ray beam incident on the film surface (through direction), the 010 reflection is predominant, whereas with the X-ray beam incident on the film edge (edge direction) the 100 reflection has the highest intensity. In the present study, only a through scan was made, permitting reliable measurement of crystallite size normal to the 010 planes using the profile-fitting procedure and the Scherrer equation [28]. Peak half-widths were corrected for instrumental broadening, but not for lattice-distortion broadening. The extent of the latter effect, if any, could not be investigated due to lack of suitable higher-order

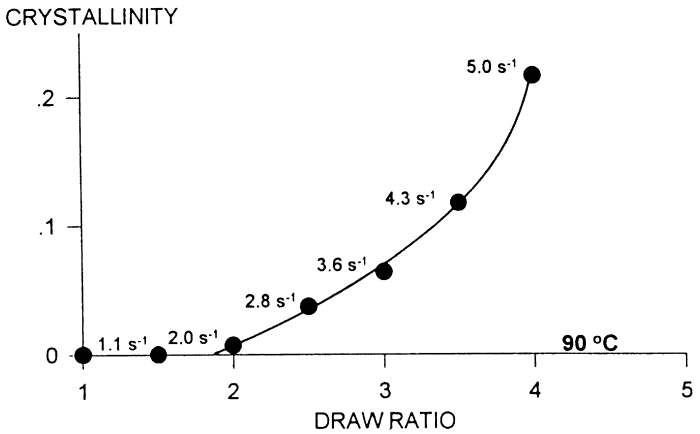

Figure 5 Volume fraction crystallinity as a function of draw ratio for CF-drawn film, in which the residence time was constant and the strain rate therefore increased with draw ratio.

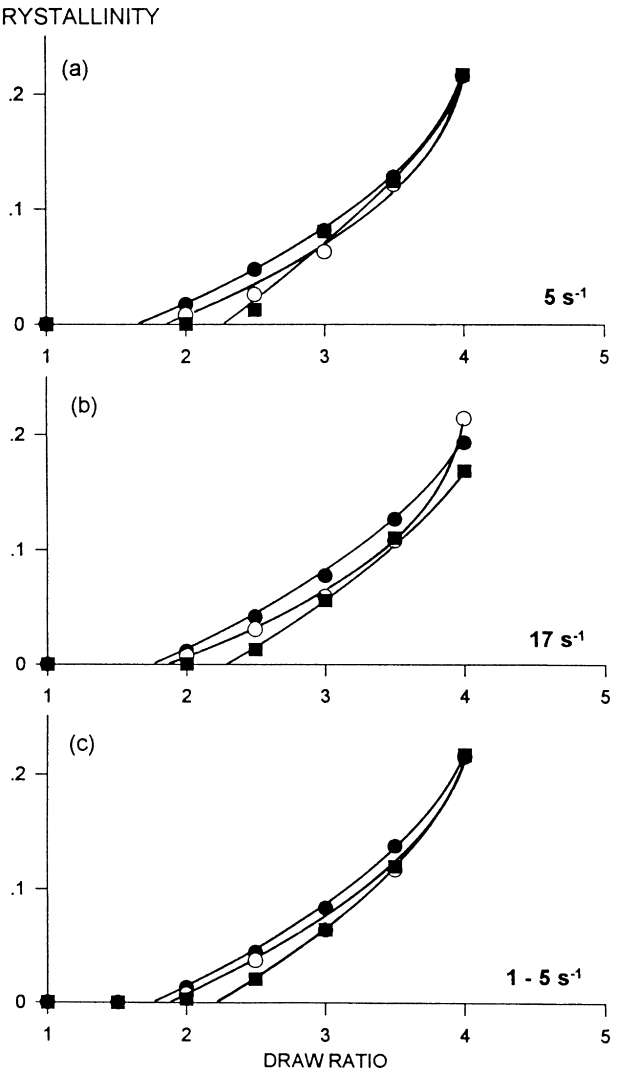

Figure 6 Volume fraction crystallinity as a function of draw ratio for CF-drawn film at draw temperatures of 83°C (●), 90°C (○) and 96°C (■), and at (average) strain rates of (a) 5 s^{-1}, (b) 17 s^{-1} and (c) variable—see *Figure 5*.

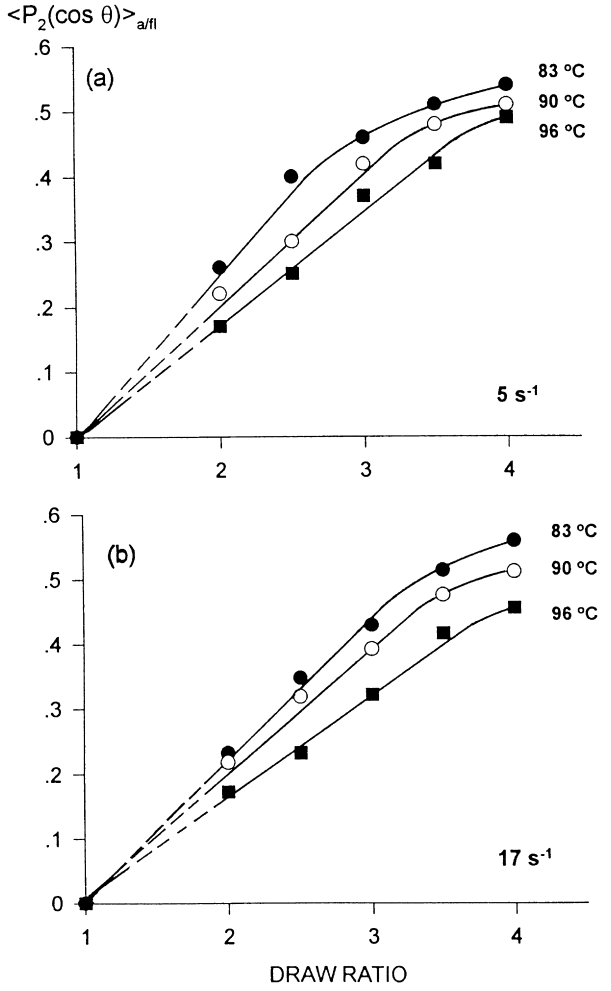

Figure 7 Non-crystalline (amorphous) orientation, obtained from polarized intrinsic fluorescence measurements, as a function of draw ratio for CF-drawn film at three draw temperatures and two strain rates.

reflections. Since in the present study we are concerned only with a first-order reflection, the contribution of lattice distortion to line breadth is likely to be small.

Specimens for WAXS analysis in the through direction were prepared by cutting segments (12×8 mm) from the drawn film, and stacking them to form a closely packed laminate 0.5 mm thick. Glue was used only on the top and bottom edges of the laminates, outside the range of the X-ray beam.

Birefringence

Optical birefringence measurements were made in the research laboratories of Hoechst Diafoil by means of an Abbé Refractometer.

RESULTS AND DISCUSSION

Development of crystallinity and 'non-crystalline orientation'

The development of crystallinity with draw ratio for roll-drawn film is shown in *Figure 4*, at draw temperatures, T_d, of 83, 90 and 96°C and (average) strain rates of 5 and 17 s^{-1}. Evidently, there is no influence of strain rate on crystallinity development in this strain-rate range. These samples were produced at a constant average strain-rate; i.e. as draw ratio increased, total line speed was reduced in order to maintain the same average strain rate. Other samples were produced with the line speed constant, so that there was a constant residence time at each draw ratio and strain rate increased with draw ratio. The crystallinity *versus* draw ratio relationships for the samples with increasing strain rate are essentially identical to those in which the average strain rate was kept constant, as shown at $T_d = 90$°C, e.g. in *Figure 5*.

Within the processing window studied, the draw temperature has a significant influence on crystallinity development. The onset of crystallization is shifted to higher draw ratios with increasing draw temperature (*Figure 6*), but as crystallinity develops the curves of crystallinity *versus* draw ratio tend to merge.

Whereas changing strain rate from 5 to 17 s^{-1} has no significant influence on the development of molecular orientation in the non-crystalline regions (i.e. the plots of *Figure 7*a and b are essentially the same), varying draw temperature has an important effect. Orientation in the non-crystalline phase $\langle P_2(\cos\theta)\rangle_{a/fl}$ (determined by the chain-intrinsic fluorescence method) increases more slowly as a function of draw ratio at higher draw temperatures, reflecting increasing rates of orientational relaxation with increasing temperature (*Figure 7*). The crystallinity values at the three temperatures come close together at the higher

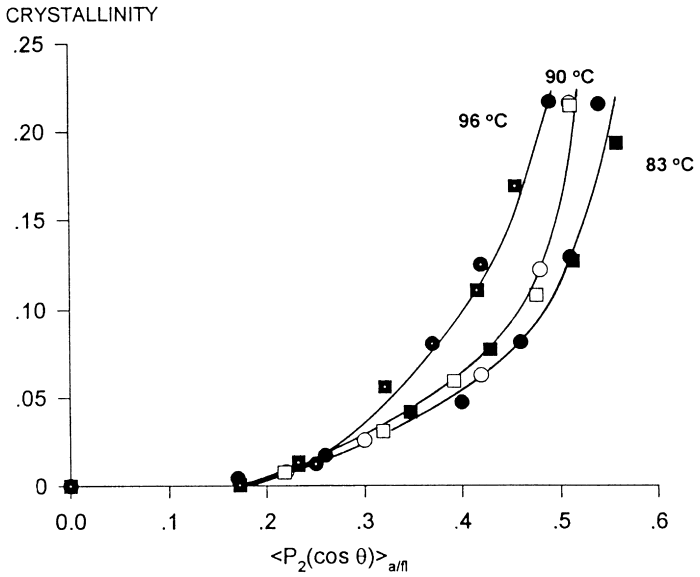

Figure 8 Volume fraction crystallinity as a function of non-crystalline orientation for CF-drawn film at three draw temperatures (and strain rates of 5 s^{-1} and 17 s^{-1}).

draw ratios (*Figure 6*) because enhanced molecular mobility at higher temperatures results in more rapid crystallization at a given level of non-crystalline orientation.

Figure 8 is a plot of crystallinity *versus* $\langle P_2(\cos\theta)\rangle_{a/fl}$ for the roll-drawn film, showing the extent to which higher temperatures result in higher crystallinities at a given level of non-crystalline orientation. It is puzzling, however, that *Figure 8* indicates the critical orientation for onset of crystallization to be independent of draw temperature, having a value of about 0.18. This is contrary to Le Bourevellec et al.'s data from film drawn at a constant strain rate [9], and contrary to our own data from film drawn at a constant extension rate [25], since both sets of data show the critical orientation decreasing with increasing draw temperature. A possible reason for this significant difference between roll drawing and constant-rate drawing will be discussed later.

The development of optical birefringence as a function of draw ratio is clearly temperature dependent (*Figure 9*). Higher draw temperatures result in lower birefringence values at a given draw ratio. Since crystallinity development (*Figure 6*) is much less temperature dependent than birefringence, the lower birefringences at higher temperature must largely reflect lower non-crystalline orientation, which confirms our chain-intrinsic fluorescence results (*Figure 7*). Making the, not very reasonable, assumption that the crystallite orientation $\langle P_2(\cos\theta)\rangle_c$ in all the samples is 0.9, and assuming intrinsic birefringence values for the crystalline and amorphous phases of 0.22 and 0.275, respectively, we have calculated orientation in the non-crystalline regions from birefringence $\langle P_2(\cos\theta)\rangle_{a/bir}$ using Stein's well-known relationship [29]. The results, given in *Figure 10*, show a trend similar to that of those obtained from the intrinsic fluorescence method, but we are sure the latter provides a much more accurate picture of non-crystalline orientation development.

Figure 11 shows equatorial WAXS scans from film roll-drawn at 90ºC to draw ratios of 3.5 and 4. Evidently, the crystalline reflections are too weak to resolve at $\lambda = 3.5$, but the 010 reflection becomes distinct at λ=4. The predominance of the 010 peak in the scan is indicative of

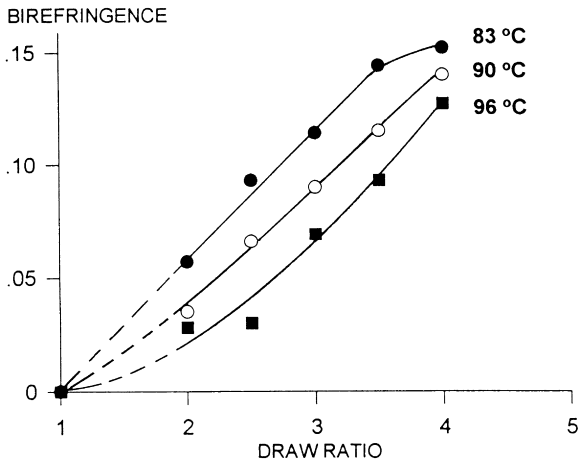

Figure 9 Optical birefringence as a function of draw ratio for CF-drawn film at three draw temperatures and an (average) strain rate of 5 s^{-1}.

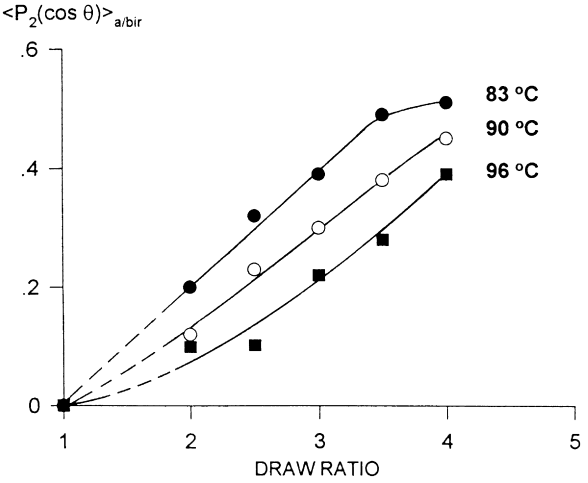

Figure 10 Non-crystalline (amorphous) orientation, estimated from the birefringence–crystallinity method, as a function of draw ratio for CF-drawn film at three draw temperatures and an (average) strain rate of 5 s^{-1}.

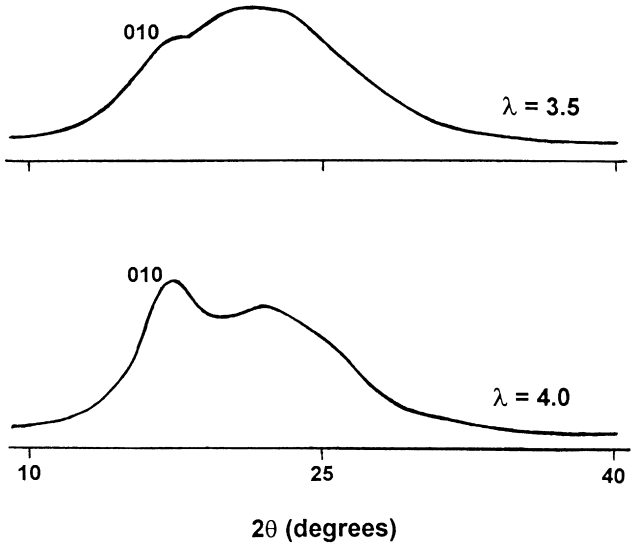

Figure 11 Equatorial WAXS scans from film CF-drawn at 90°C to draw ratios of 3.5 and 4.0. The X-ray beam was incident on the film surface (through direction), permitting determination of crystallite size normal to the 010 planes.

significant planar orientation of the crystals, with the 100 plane tending to align with the film surface. Crystal size normal to the 010 planes in the λ=4 sample is 3.3 nm, which is very similar to the crystal sizes we reported for CER-drawn samples in the second crystallization regime [6].

Comparison of constant-force (CF) and constant-extension rate (CER) drawing

Due to the complex strain-rate history of roll-drawn (or CF-drawn) film, comparison of its structure with that of film drawn at a constant extension rate is problematic. *Figure 12* compares crystallinity development at 90ºC for CER-drawn film at strain rates of 0.42 and 0.01 s^{-1} with roll-drawn film at an average strain rate of 5 s^{-1}. For CER drawing, it is well established that increasing strain rate shifts the onset of crystallization to lower draw ratios, because reduced time available for relaxation of non-crystalline orientation causes the critical orientation for crystallization onset to be reached earlier [6,9,10,15–17]. Therefore, due to its higher average strain rate, one would expect the curve for the roll-drawn film to lie on the low draw ratio side of the 0.42 s^{-1} (CER-drawn) curve, whereas it actually lies on the high draw ratio side. On the other hand, the development of non-crystalline orientation in the roll-drawn film is more rapid than that in the 0.42 s^{-1} CER-drawn film (*Figure 13*), which is an expected result of the reduced time available for relaxation of orientation. Consequently, a plot of crystallinity *versus* $\langle P_2(\cos\theta)\rangle_{a/fl}$ shows that roll drawing produces a much lower degree of crystallinity for a given level of non-crystalline orientation (*Figure 14*). In order to attempt an explanation for this phenomenon, we need to consider the kinetics of deformation during roll drawing.

Le Bourvellec et al. [11] found that drawing under constant load results in curves of draw ratio *versus* draw time which end in a plateau. The plateau occurs because crystallinity induced during drawing increases the modulus of the polymer to a point where deformation can no longer continue under the applied load. In roll drawing, the film chooses its deformation kinetics such that the applied draw ratio is attained under the minimum necessary force. For a given temperature and given draw ratio, there is a minimum time, t_p, needed to reach the plateau deformation. A residence time between rolls greater than t_p gives the film enough time to reach the plateau deformation under the minimum drawing force. A residence time less than t_p causes the film to be drawn faster under a higher force, resulting in a plateau deformation higher than the applied draw ratio. The strain rate passes through a maximum, reaching zero at the onset of the plateau [11].

Constant-load experiments have shown that the strain-rate maximum occurs somewhat after crystallization begins [13], so the rate of deformation just before crystallization onset, and throughout the early part of crystallization, is considerably higher than the average strain rate for the total deformation. We believe, therefore, that in the region of the strain-rate maximum, the time available for crystallization becomes so short that the level of crystallinity at a given

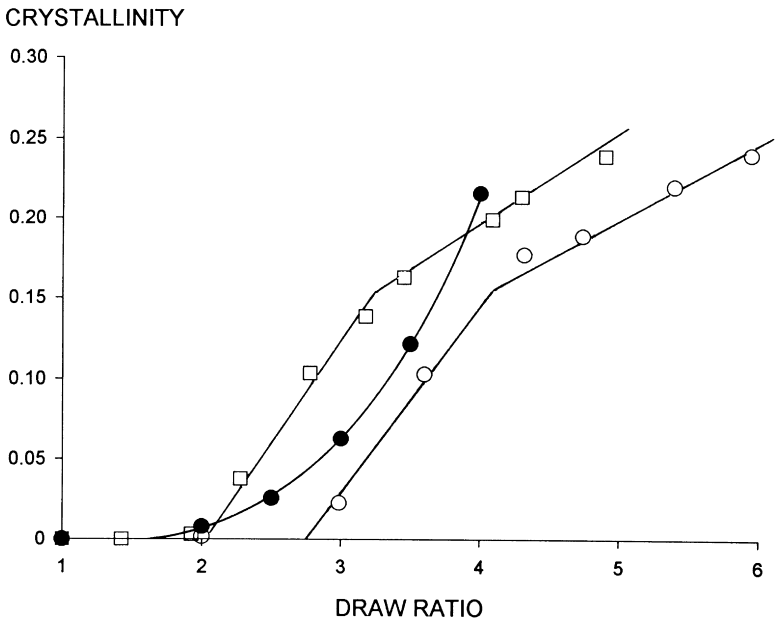

Figure 12 Volume fraction crystallinity *versus* draw ratio for film CF-drawn at 90°C at an (average) strain rate of 5 s^{-1} (●), compared with film CER-drawn at 90°C at strain rates of 0.42 s^{-1} (□) and 0.02 s^{-1} (○).

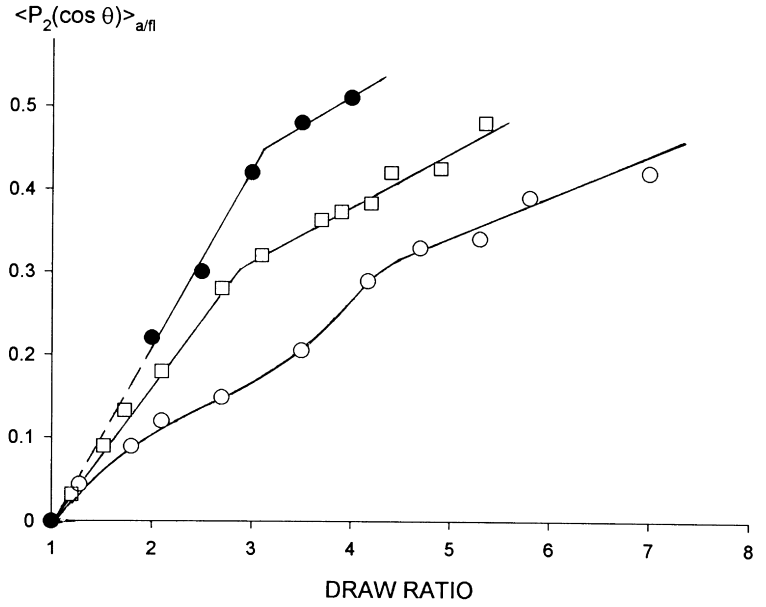

Figure 13 Non-crystalline (amorphous) orientation *versus* draw ratio for film CF-drawn at 90°C at an (average) strain rate of 5 s^{-1} (●), compared with film CER-drawn at 90°C at strain rates of 0.42 s^{-1} (□) and 0.02 s^{-1} (○).

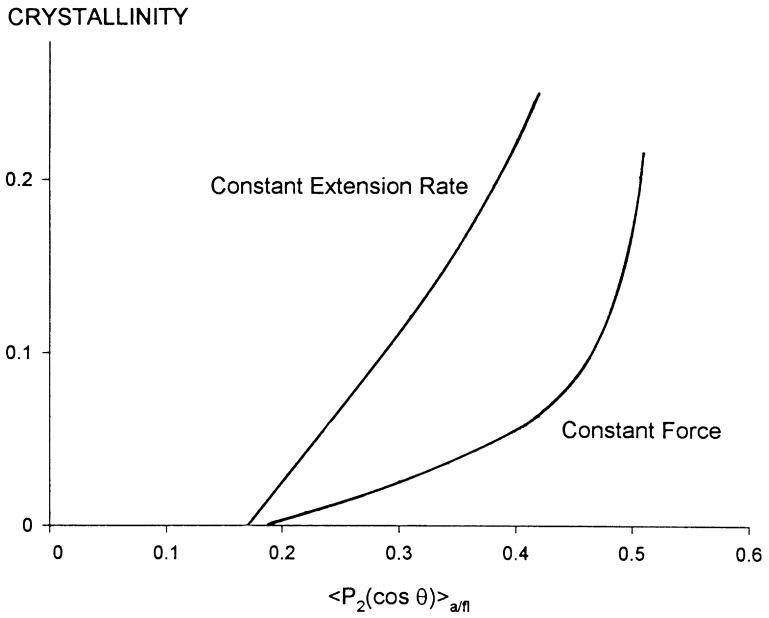

Figure 14 Volume fraction crystallinity *versus* non-crystalline orientation for CER drawing and CF drawing at 90°C. The nominal strain rate for CER drawing was 0.01 s^{-1}. The CF curve is from data obtained at (average) strain rates of 5 and 17 s^{-1}.

level of non-crystalline orientation is severely reduced. In the lower strain-rate range associated with constant extension-rate drawing, the main impact of increasing strain rate is to reduce the time available for orientational relaxation without much influencing the degree of crystallinity attained at a given level of orientation. At the very high strain rates reached in roll drawing, however, orientational relaxation may start to become relatively insensitive to changes in strain rate, while the development of crystallinity at a given level of orientation may become more sensitive. It is well known that the rate of crystallization in oriented PET is greatest at very short times (see, e.g. Refs 30–32), while the rates of stress relaxation and, presumably, orientational relaxation, become increasingly negligible at short times. (Being a constant-force deformation, no stress relaxation occurs of course. However, the effectiveness with which the applied force orients the chains will depend on the time available for orientational relaxation.)

Figure 15 illustrates schematically the relative time dependences of crystallization and orientational relaxation. In region B, reducing time (increasing strain rate) would substantially decrease the amount of orientational relaxation that can take place, but would have little effect on the degree of crystallinity attained at a particular level of orientation. Thus, in region B, the level of non-crystalline orientation at a given draw ratio increases with strain rate, whereas the level of crystallinity is determined only by the level of non-crystalline orientation and not by the strain rate. This is consistent with the development of orientation and crystallinity observed in our CER studies. In region A, increasing strain rate would reduce the level of crystallinity attained at

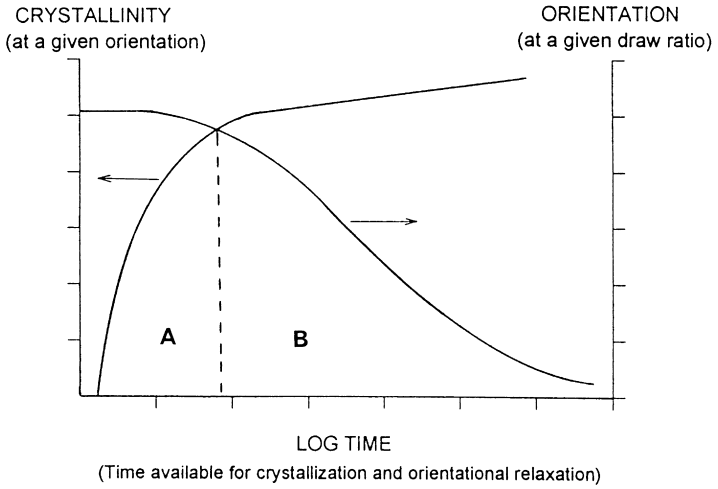

Figure 15 Schematic indicating the influence of time available during drawing on crystallization and on orientational relaxation in the non-crystalline phase.

a particular level of non-crystalline orientation, but would no longer increase non-crystalline orientation at a given draw ratio. The fact that roll-drawn film displays lower levels of crystallinity at a given level of orientation than CER-drawn film (*Figure 14*), and the fact that non-crystalline orientation is essentially unchanged when strain rate is increased from 5 to 17 s^{-1} (*Figure 7*), indicates that much of the constant-force deformation takes place in a regime similar to A.

These arguments clearly require that there is a pseudo-equilibrium crystallinity level associated with a particular level of non-crystalline orientation. In CER drawing, there is enough time available for crystallization to reach the pseudo-equilibrium level, whereas in the high-strain-rate region of CF drawing there is insufficient time to reach this level. The notion of a pseudo-equilibrium crystallinity level which increases with the degree of non-crystalline orientation is consistent with the (low strain rate) CSR data of Le Bourevellec et al. [10], who showed that after drawing to any draw ratio, the rate of crystallization during subsequent constant-length annealing at the draw temperature is small, or even negligible, compared to the rate of crystallization during the drawing process. Thus, when the strain rate is sufficiently low, the development of crystallinity is predominantly controlled by the level of non-crystalline orientation and not by the time available for crystallization. Although the pseudo-equilibrium crystallinity level increases with the level of non-crystalline orientation, it is likely that at sufficiently long annealing times, a true equilibrium crystallinity level is reached which is not dependent on the degree of non-crystalline orientation, as indicated, e.g. in the higher temperature crystallization data of Alfonso et al. [32].

Our interpretation of the CF and CER crystallinity results is supported by the data in *Figure 16*a. The open squares are the crystallinity (χ) *versus* draw ratio (λ) data for 90°C roll-drawn (CF) film. The filled circles are the crystallinity values of these films after constant-length reheating to 90°C in the Instron furnace and air-quenching. It is interesting that after reheating the roll-drawn films, both the curve shape and crystallinity levels become remarkably similar to those obtained in CER drawing. *Figure 16*b compares the χ *versus* λ curve for CER-drawn film at a strain rate, $\dot{\epsilon}$, of 0.42 s^{-1} with that of the roll-drawn film ($\dot{\epsilon} = 5\ s^{-1}$) after reheating to 90°C. Not only are the curve shapes and crystallinity levels similar, but the curve for roll-drawn film is shifted

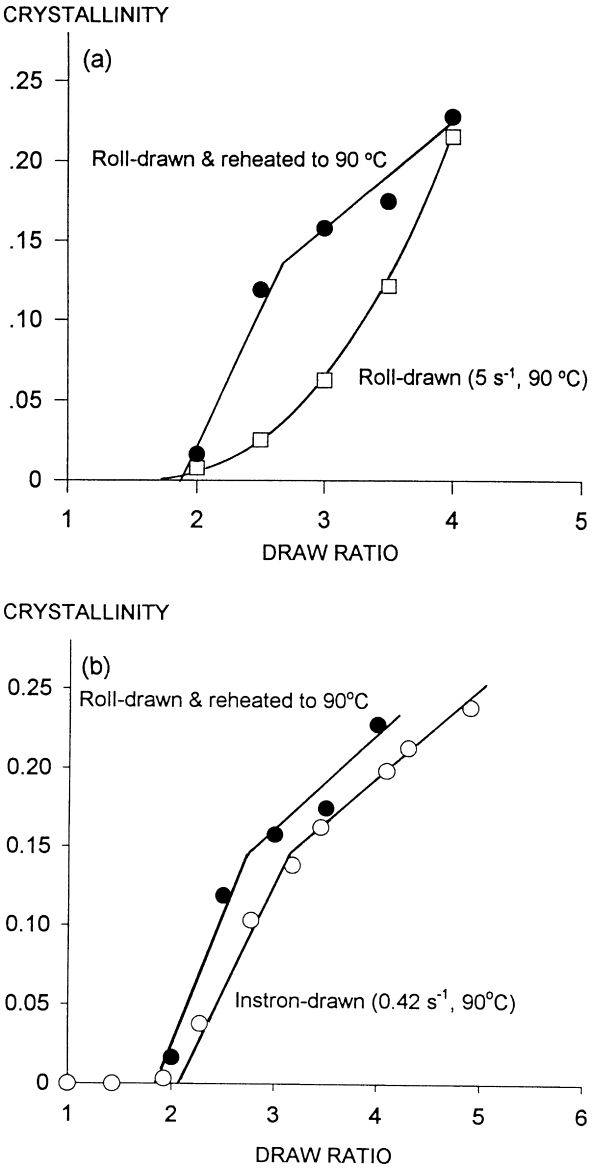

Figure 16 (a) Crystallinity *versus* draw ratio for film CF-drawn (roll-drawn) at 90°C (●), and for the same films after (isometric) reheating in an Instron furnace to 90°C (□). (b) Comparison of the crystallinity *versus* draw ratio relationship for the reheated CF-drawn films, where average strain rate was 5 s^{-1}, with CER-drawn (Instron) films, where nominal strain rate was 0.42 s^{-1}.

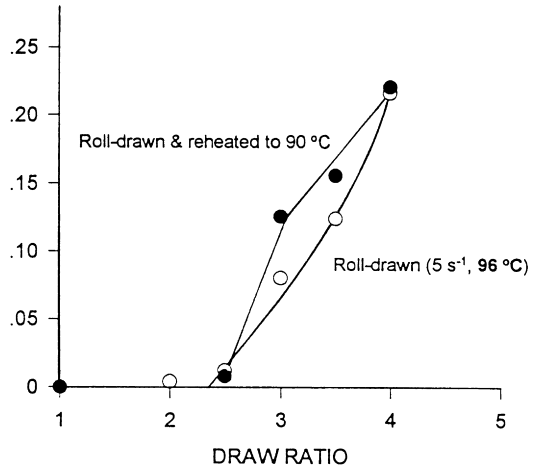

Figure 17 Crystallinity *versus* draw ratio for film CF-drawn (roll-drawn) at 96°C (●), and for the same films after (isometric) reheating in an Instron furnace to 90°C (□).

somewhat to lower draw ratios, which is consistent with our CER data showing the χ *versus* λ curves shifting to lower λ with increasing strain rate. It is especially noteworthy that the change in slope associated with the onset of regime 2 crystallization [6,15,16] becomes apparent in the roll-drawn film after reheating and, as with CER drawing, occurs at a crystallinity level of 0.15. These data confirm that in the high strain rate region of CF drawing, pseudo-equilibrium crystallinity values are not reached, and that subsequent annealing at the draw temperature permits an increase in crystallinity values to pseudo-equilibrium levels. A further example of this phenomenon is shown in *Figure 17*. In this case, the temperature during roll drawing was 96ºC, and the reheat temperature was, again, 90ºC. The fact that the increase in crystallinity is substantially less than was observed when the film roll-drawn at 90°C was reheated to 90°C (*Figure 16*) is consistent with the lower levels of non-crystalline orientation at the higher draw temperature (see *Figure 7*): i.e. a lower orientation level provides a lower pseudo-equilibrium crystallinity level.

It is interesting that at the highest draw ratio of 4, crystallinity increases quite sharply (*Figures 4–6*), and the crystallinity level is similar to that obtained from constant extension rate drawing (*Figure 12*). This may be because, at the highest draw ratio, the final stages of stress-induced crystallization occur at the tail-end of the strain-rate spectrum. The lower strain rates in this region of the spectrum would allow greater time for crystallization and a higher degree of crystallinity. It may even be that the deformation has entered the plateau region for a short time, resulting in a degree of constant-length annealing.

Another possible explanation for the lower levels of crystallinity at a given level of $\langle P_2(\cos\theta)\rangle_{a/fl}$ in the roll-drawn samples is the quenching conditions. Although it is very rapid, air-quenching after Instron drawing may not be fast enough to completely suppress crystallization during cooling. Since quenching in the roll-drawing process occurs on contact with the fast roll which is cold, cooling may be faster and, therefore, more effective at preventing crystallization during the quench. This explanation is unlikely, however, because similar (low) crystallinity levels were found in films that were air-quenched after (dead-weight) constant-load drawing in a laboratory furnace [11].

We will now turn to a more detailed discussion of the influence of draw temperature on structure development

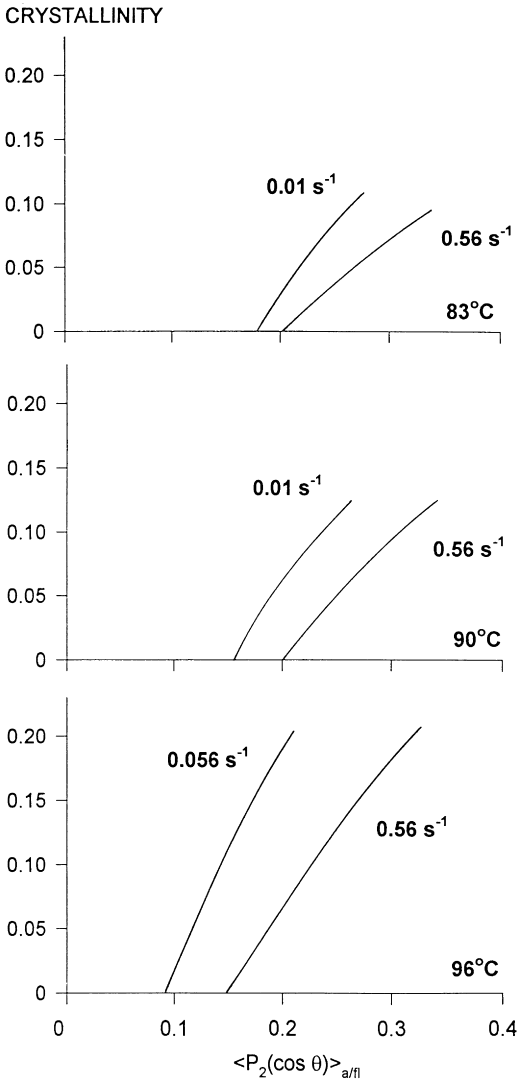

Figure 18 Influence of draw temperature and strain rate on the relationship between volume fraction crystallinity and non-crystalline orientation. Note that these data were obtained from samples drawn in uniaxial extension (unrestrained), whereas the rest of the data in this paper were obtained from samples drawn in pure shear (constant width)—see Experimental Section.

during roll drawing. For CER drawing, it has been reported that the draw ratio for onset of crystallization λ_c increases with draw temperature [9,20], because higher temperatures increase the rate of orientational relaxation. We have shown, however, that at sufficiently high strain rates, increasing temperature shifts λ_c to lower draw ratios (see figures 2 and 12 of Ref. 17). This is because higher temperatures not only increase the rate of orientational relaxation, but also enhance the rate of crystallization at a given level of non-crystalline orientation and reduce the critical orientation for onset of crystallization. Thus, when the time available for relaxation becomes very short, at high strain rates, the effect of enhanced crystallization rate dominates. In view of the high strain rates at which the roll-drawn samples were produced, we would have expected λ_c at 96ºC to have been somewhat lower than λ_c at 83 and 90ºC [17], whereas it is actually higher. This behaviour is connected to the fact that the critical orientation for the onset of crystallization seems to be independent of draw temperature in the roll-drawn samples (*Figure 8*). If the critical orientation for crystallization had decreased significantly

with increasing draw temperature, as occurs in CER drawing, crystallization onset in the roll-drawn films would indeed have occurred at a lower draw ratio for $T_d = 96$ºC than for $T_d = 90$ºC.

As crystallization progresses during roll drawing, the level of crystallinity at a given level of $\langle P_2(\cos\theta)\rangle_{a/fl}$ is higher at higher temperatures (*Figure 8*), as expected; so why is the critical orientation for crystallization onset independent of T_d? A possible explanation is that strain rate in the region of crystallization onset might be significantly higher at higher draw temperatures [13], such that the time is too short to permit induction of crystallinity at the critical orientation associated with lower strain rates. In other words, the critical orientation is both strain-rate and temperature dependent, increasing with increasing strain rate and decreasing with increasing temperature. It turns out that there is in fact evidence for this in our CER data. Based on plots of $\langle P_2(\cos\theta)\rangle_{a/fl}$ *versus* draw ratio (and also on the data of Le Bourvellec et al. [9]), we had previously inferred that the critical orientation for induction of crystallinity was independent of strain rate in CER drawing [15]. However, the critical orientation is more accurately obtained from plots of $\langle P_2(\cos\theta)\rangle_{a/fl}$ *versus* crystallinity (*Figure 18*), from which it seems that the critical orientation is always somewhat higher at the strain rate of 0.56 s^{-1} than at the lower strain rate. The plots at 83 and 96ºC were generated from orientation and crystallinity data that will be published elsewhere [26], together with some further discussion of the trends shown in *Figure 18*.

Comparison with real time X-ray studies

In a real-time X-ray study involving high deformation rates (~10 s^{-1}) at temperatures between 80 and 110ºC, Blundell et al.[33] recently found that much of the crystallinity that was induced as a result of drawing developed within about 200 ms after reaching the final draw ratio of 4, with relatively little crystallization occurring before this final extension. These results are entirely consistent with the present high-strain-rate study, confirming that sufficient time is required to reach the pseudo-equilibrium crystallinity level and that, at high strain rates, very low levels of crystallinity (essentially undetectable by X-ray diffraction) are generated at draw ratios below 4. The low levels of crystallinity obtained in our roll-drawing experiments demonstrate that the quenching conditions, on the chill roll, were rapid enough and occurred sufficiently close to the end of drawing to prevent post-draw crystallization. At a draw ratio of 4, crystallinity reached the pseudo-equilibrium level because, in roll-drawing, microstructural evolution causes the strain rate to slow down to the point where this becomes possible. In this connection, it may be noted that although the strain rates used in the study of Blundell et al.[33] were relatively high, they were at a constant rate of extension (or possibly a constant strain rate) and therefore did not involve the strain-rate history characteristic of commercial (constant-force) drawing.

For fast-drawn samples, where the time-scale of the deformation can be faster than the time to reach pseudo-equilibrium crystallinity levels, the quenching conditions are certainly much more critical than for slow-drawn samples, and the studies of Blundell et al. confirm that the quenching conditions of the present study are suitable for obtaining reliable crystallinity data that are consistent with real-time analysis.

CONCLUSIONS

Previous studies on CER and CSR drawing of PET film [6,10,14–19] have shown that at strain rates ≤ 2 s^{-1} and temperatures between 80 and 100°C, microstructure development is strongly influenced by the time available for molecular relaxation. The time available for relaxation controls the level of molecular orientation attained at a given draw ratio which, in turn, determines the degree of crystallinity that can develop at a given temperature. This is because crystallization is fast relative to the time-scale of the deformation and there is always time to reach the pseudo-equilibrium crystallinity level corresponding to a particular combination of non-crystalline orientation and temperature.

It is known that in CF drawing in the temperature range 80–100°C, strain rate passes through a maximum in the course of the deformation (unless the deformation is stopped before the maximum is reached) [11,13]. Thus, CF drawing at some *average* strain rate involves an excursion to strain rates that can be an order of magnitude higher than the average value. The present study strongly indicates that in the region of the strain-rate maximum, during which crystallization takes place, there is insufficient time for crystallinity to reach pseudo-equilibrium levels associated with a given level of non-crystalline orientation. Also, since the high strain rates in CF drawing reduce the time available for relaxation of orientation, non-crystalline orientation evolves more rapidly than in CER drawing.

ACKNOWLEDGEMENTS

These studies were undertaken in connection with the TRI project ‘Structure and Properties of Poly(ethylene Terephthalate) Film’, supported by a group of TRI participants including DuPont, Goodyear, Hoechst Diafoil, 3M and Toray. The author thanks Dr Gregory Farell of Hoechst Diafoil for preparing the roll-drawn samples, supervising the birefringence measurements and providing valuable information on the commercial film-drawing process. The author is also indebted to Lei Zhang and Dennis W. Briant for their careful experimental work.

REFERENCES

1. Foster, E. L. and Heap, H., *Br. J. Appl. Phys.*, 1957, **8**, 400.
2. Thompson, A. B., *J. Polym. Sci.*, 1959, **34**, 741.
3. Reitsch, F., Duckett, R. A. and Ward, I. M., *Polymer*, 1979, **20**, 1133.
4. Ward, I. M., *Polym. Engng Sci.*, 1984, **24**, 724.
5. Long, S. D. and Ward, I. M., *J. Appl. Polym. Sci.*, 1991, **42**, 1921.
6. Salem, D. R., *Polymer*, 1992, **33**, 3182.
7. Buckley, C. P., Jones, D. C. and Jones, D. P., *Polymer*, 1996, **37**, 2403.
8. Gordon, D. H., Duckett, R. A. and Ward, I. M., *Polymer*, 1994, **35**, 2554.
9. Le Bourvellec, G., Monnerie, L. and Jarry, J. P., *Polymer*, 1986, **27**, 856.
10. Le Bourvellec, G., Monnerie, L. and Jarry, J. P., *Polymer*, 1987, **28**, 1712.
11. Le Bourvellec, G., Beautemps, J. and Jarry, J. P., *J. Appl. Polym. Sci.*, 1990, **39**, 319.
12. Lorentz, G. and Tassin, J. F., *Polymer*, 1994, **35**, 3200.
13. Le Bourvellec, G. and Beautemps, J., *J. Appl. Polym. Sci.*, 1990, **39**, 329.
14. Salem, D. R., *Polymer*, 1992, **33**, 3189.
15. Clauss, B. and Salem, D. R., *Polymer*, 1992, **33**, 3193.
16. Clauss, B. and Salem, D. R., *Macromolecules*, 1995, **28**, 8328.
17. Salem, D. R., *Polymer*, 1994, **35**, 771.
18. Salem, D. R., *Polymer*, 1995, **36**, 3605.

19. Salem, D. R., (To be published). An abbreviated version appears in *Book of Abstracts: Ninth Annual Meeting of the Polymer Processing Society*, Manchester, UK, 1993, p. 83.
20. Spruiell, J. E., McCord, D. E. and Beuerlein, R. A., *Trans. Soc. Rheol.*, 1972, **16**, 535.
21. Heuvel, H. M. and Huisman, R., *J. Appl. Polym. Sci.*, 1978, **22**, 2229.
22. Parker, J. P. and Lindemeyer, *J. Appl. Polym. Sci.*, 1977, **21**, 821.
23. Salem, D. R., Moore, R. A. F. and Weigmann, H.-D., *J. Polym. Sci. Polym. Phys. Edn*, 1987, **25**, 567.
24. Salem, D. R., *J. Polym. Sci. Polym. Phys. Edn*, 1987, **25**, 2561.
25. Nobbs, J. H., Bower, D. I. and Ward, I. M., *Polymer*, 1976, **17**, 25.
26. Salem, D. R., To be published.
27. Heuvel, H. M., Huisman, R. and Lind, K. C. J. B., *J. Polym. Sci. Polym. Phys. Edn*, 1976, **14**, 921.
28. Cullity, B. D., *Elements of X-Ray Diffraction*, Chapter 3, Addison-Wesley, London, 1967, pp. 96–99.
29. Stein, R. S., *J. Polym. Sci. A2*, 1968, 6, 1975.
30. Smith, F. S. and Steward, R. D., *Polymer*, 1974, **15**, 283.
31. Peszkin, P. N., Schultz, J. M. and Lin, J. S., *J. Polym. Sci. Polym. Phys. Edn*, 1986, **24**, 2591.
32. Alfonso, G. C., Verdona, M. P. and Wasiak, A., *Polymer*, 1978, **19**, 711.
33. Blundell, D. J., MacKerron, D. H., Fuller, W., Mahendrasingam, A., Martin, C., Oldman, R. J., Rule, R. J. and Riekel, C., *Polymer*, 1996, **37**, 3303.